International Journal of Applied Engineering Research ISSN 0973-4562 Volume 12, Number 24 (2017) pp. 15610-15620

Use of Digital Aerial Photogrammetry Sensors for Land Cover Classification

Massimiliano Pepe[1]

[1]*Department of Sciences and Technologies, University of Naples "Parthenope", Italy.*
Orcid Id: 0000-0003-2508-5066

Abstract

The modern digital photogrammetric sensors are increasingly popular even in Remote Sensing (RS) field thanks to their ability to acquire in very high resolution and in Multi-Spectral (MS) mode: red, green, blue and in the Near Infrared (NIR) band. In addition, the trend, begun with large-format digital photogrammetric cameras, has also been applied to develop even medium and small format sensors in order to obtain a high geometric resolution of the images. Indeed, depending on the constructional features, these sensors can be mounted on airborne or Unmanned Aerial Vehicle (UAV) platforms. The aim of the paper is to investigate potentiality MS bands, generated by photogrammetric sensors, in order to build land cover maps. The presence of the NIR band is particularly useful for describing vegetation as through the indices it is possible to clearly distinguish vegetation from other elements present in the image. For the determination of land use classes, according to the "Corine Land Cover" (CLC) standard, an approach that combines remote sensing techniques with the classical ones of photo-interpretation has been experimented. In fact, not all objects of the territory can be recognized in an automatic way, but a reading key is necessary and only the knowledge of the territory can be established by the photo interpreter, such as for some artificial classes. In this paper, a case study on the use of MS image obtained airborne sensor is presented. In particular, using Z/I Imaging Digital Mapping Camera DMC® (manufactured by Intergraph), it has been possible to acquire in MS mode on a specific test area and subsequently, to realize using CLC of the IV level the land cover map with elevated detail.

Keywords: Airborne sensors, land cover map, thematic map, NIR, Digital Number.

INTRODUCTION

The benefit of the use of the Infrared band in the field of Photogrammetry and Remote Sensing (Pa&RS) for the study of the vegetation and, more in general the classification of land object, has been well known for a long time. The first study (around the 1956) was conducted by Colwell on the use of CIR (Colored InfraRed) for the classification and recognition of vegetation types and the detection of diseased and damaged or stressed vegetation. Of course, this experience, along with other successive research is related to the use of photosensitive material, such as the infrared film [1, 2]. However, the use of these films required particular photogrammetric flights and special procedures in order to obtain a good quality of the photo. Indeed, the infrared colour films are very sensitive to changes in temperature and humidity during aerial survey. In addition, the sensitivity of the film (which it difficult to control even in a manufacturing laboratory) deteriorates over time and requires optimum storage conditions [3].

With the advent of CCD (Charge-Coupled Device) or CMSOS (Complementary Metal-Oxide Semiconductor) chips, the solid-devices convert the light into electrons in a radiometric value [4]. So, the modern digital sensors can be acquiring in separate bands in Red, Green, Blue and Infrared and as a consequence, it is possible to obtain true and false colour images as the same time [5]. The digital sensors for PaRS purpose, can be used in variety of airborne configurations. Two principal airborne digital imaging technologies are frame cameras and push-broom line scanners. In the first group, there are the sensors that construct the central prospective and in relation to size of the sensors, it is possible distinguish in small, media and large format. In the second group belong the sensors characteristic is to produce continuous strip imagery of the terrain [6].

These sensors can be used, beyond the traditional products, such as stereoscopy cartography and colour orthophotos, in forest application in order to distinguish the type of the vegetation [7], archaeological prospection [8], in the planning and governance issues [9] and land cover classification [10]. In recent years, especially the classification of the territory objects by remote sensing platform, is becoming widespread [11, 12]. In land cover application, a standard of classification is the so-called Corine Land Cover (CLC), which is referring to a European programme establishing a computerised inventory on land cover of the 27 EC member states and other European countries. In Italy, a thematic deepening of database Corine Land Cover 2006 for some classes of the CORINE nomenclature system, mainly for the class "wooded areas and semi-natural environments"has been created [13]. Considering the initial scale of representation of this project (1:100.000), the develop of land cover classification has been addressed mainly through the use of multispectral sensors mounted on board satellite platform [14, 15]. However, increasing the level of the detail of the territory, the need to represent land use with a high degree of detail, is conducting research into the use of suitable sensors mounted on airborne or UAV [16].

In order to show the applications of the multispectral images generate by airborne sensors for land cover purpose, the paper has been organized in several section. The section called "Remote Sensing by aerial digital photogrammetry sensor" illustrates the potential of the multispectral images generated

by photogrammetric camera. Indeed, by the use of different bands and their combination it is possible to derive vegetation indices (VI) and other important indexes helpful in Remote Sensing applications. Subsequently, the procedure for converting values from Digital Number to reflectance is designated. Section "data and methods" explains, by a case study, the high detail of thematic map realized. Considerations and conclusions are summarized at the end of the paper.

USE OF REMOTE SENSING BY AERIAL DIGITAL PHOTOGRAMMETRY SENSOR

The digital photogrammetry sensor allows the acquisition in panchromatic (PAN) and in multispectral (MS) mode. Acquiring in multispectral mode, it is possible to use the characteristics of each band. Following, a short description of the single band and their benefit in land use analysis, is reported [17, 18].

Blue band: The lower limit corresponds to the clear water transmission peak and therefore the blue band is suitable for the study of the transparency of the water and the presence of suspended material. In this wavelength, it is possible to observe changes related to the chlorophyll/carotenoid ratio and thus stress phenomena.

Green Band: This band coats the spectrum between the two chlorophyll absorption regions and, consequently, plants that reflect greenness are a healthy and vigorous vegetation. The relationship between the blue and green stripes provides information on dissolved organic matter and the presence of plankton in a water body.

Red band: This is the reference band for geometric controls as, as the atmospheric diffusion is lower than in the rest of the visible, the surface shapes exhibit a high contrast and at the same time provides a clear separation between vegetated areas and uncovered soils. It is also extremely important for its sensitivity to chlorophyll concentration in vegetation.

Infrared or IR band: This band is essential to follow the evolution of the state of vegetation, as the infrared reflection peak is directly linked to the presence of leaf biomass. In addition, the reflection in this region is closely related to the nitrogen content of the leaf system. The determination of this factor is an important parameter in the study of the bio-geo-chemical cycle of terrestrial ecosystems. The variation of the reflection can be useful for discriminating between the different species [19].

In addition, based on the relationship between the several bands, various *indices* have been developed in scientific literature, as shown in the Table I. These indexes, generally expressed by a simple mathematical formula, provide specific information on the type and status (in terms of greenness or moisture) of the vegetation, water environment etc. Furthermore, some indexes can be used for land classification. For example, in the case of NDVI (Normalized Difference Vegetation Index) index, its range values are -1 to 1: negative values represent water, values around zero represent bare soil and values around 1 represent dense green vegetation. Another important index used in RS application is the NDWI (normalized difference water index) because it allows to recognize easy the water bodies and can varies from -1 to 1; values larger than 0.5 mean water bodies.

Table I. Various remote sensing indexes can be applied to MS images.

Index	Formula	N.	Reference
NDVI (Normalized Difference Vegetation Index)	$\frac{NIR - red}{NIR + red}$	(1)	[20]
NDWI *(normalized difference water index)*	$\frac{green - NIR}{green + NIR}$	(2)	[21]
Green NDVI	$\frac{NIR - green}{NIR + green}$	(3)	[22]
Simple Ratio (SR)	$\frac{NIR}{red}$	(4)	[23]
Greenness Index	$\frac{green}{red}$	(5)	[24]
ANVI (Advanced Normalised Vegetation Index)	$ANVI = \frac{NIR - blue}{NIR + blue}$	(6)	[25]

A digital imaging sensor measures incoming radiance of several bands and stores the result of the measurement as a Digital Number (DN). The sensor optics transfer the radiance entering the sensor to the detector focal plane where the image is formed. The electronic signal (obtained in a certain band) is amplified electronically using appropriate gain and offset values and filtered by the electronic point spread function. Finally, the amplified and filtered signal is sampled and quantized to DNs [26]. However, many factors affect (atmosphere, flight mission, sensor setting) can be influence the properties of airborne images [27]. Therefore, in order to obtain accuracy and repeatability measures, the sensors require a calibration procedure.

In the hypothesis of sensors that use a linear detector response, the equation that allows the conversion from the digital number DN into "at-sensor radiance" is [28]:

$$L_{tb} = cal\_gain \cdot DN_{tb} + cal\_offset_b \qquad (7)$$

where

L_{tb} -average radiance value (at sensor)

cal_gain -parameter of the linear calibration models for band b;

cal_offset_b -parameter of the linear calibration models for band b;

DN_{tb} - average DN calculated in an appropriate image window for target for band b.

In the hypothesis of knowing all the parameters for the calibration procedure, assuming that the surface is of uniform Lambertian reflectance and the atmosphere is horizontally uniform and varied, the reflected solar radiation can be calculated by (Gao, 2000):

$$\rho = \frac{\pi \cdot d^2 \cdot L_{tb}}{E \cdot \cos \vartheta_s} \quad (8)$$

Where

L_{tb} sensor radiance;

E Extra-terrestrial solar irradiance;

ϑ_s solar zenith angle;

d Earth-Sun distance (expressed in astronomical units).

In general, the values of extra-terrestrial solar irradiance are tabulated, while the Earth-Sun distance can be calculated by following approximate expression:

$$d = 1 - 0.016729 \cdot \cos\left[0.9856(\text{Julian day} - 4)\right] \quad (9)$$

Therefore, using reflectance value (see equation 8) it is possible to calculate the several indexes, such as those indicated in the Table 1.

However, each image generated by frame camera sensor has a specific value of f-stop. This value can be very different along the same acquiring direction. While for satellite based systems, the absolute radiometric coefficient is a single number, for aerial digital cameras, the aperture setting (f-number or f-stop) and the integration time should be considered [30]. In addition, because it is not easy to get the calibration parameters and extraterrestrial solar irradiance values, the transformation from DN to reflectance with appropriate precision it is quite complicated. Therefore, using the DN's values, it is not possible to compare the several indexes with other (different) sensors, such as satellite images. For example, considering the relationship between the vegetation index and the target brightness, especially in the area with dark vegetation (such as woods and forests) the NDVI value take a lower value than light surface, such as grass [18].

DATA AND METHOD

A. Study area and flight planning parameters

The area of interest (AOI) concerning a small town to the south of Italy, in the province of Salerno and in particular in the south edge of the hills overlooking the "Valley of the Sele" (Fig. 1a). Most of the territory is formed by the alluvial plain of the Sele river, which borders it eastwards. This area is characterized by intensive agricultural activity while the remaining part of the territory, positioned in the north part of the AOI, is formed by hills (Fig. 1b). At the base of the hilly system lies the urban area with its productive settlements. The study area is extended for about 15,000 hectares (15kmq).

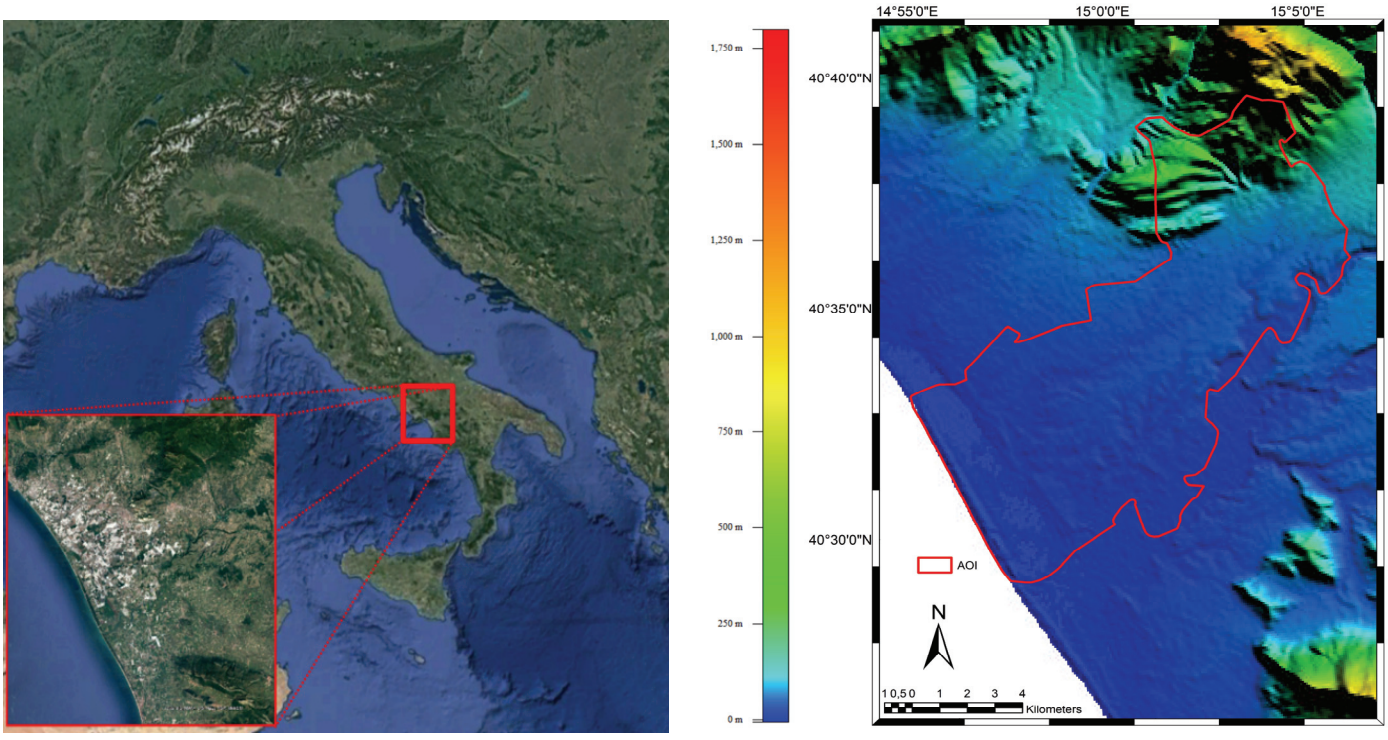

(a) **(b)**

Figure 1: Study area, a) Representation on Google Earth® - b) morphology of AOI.

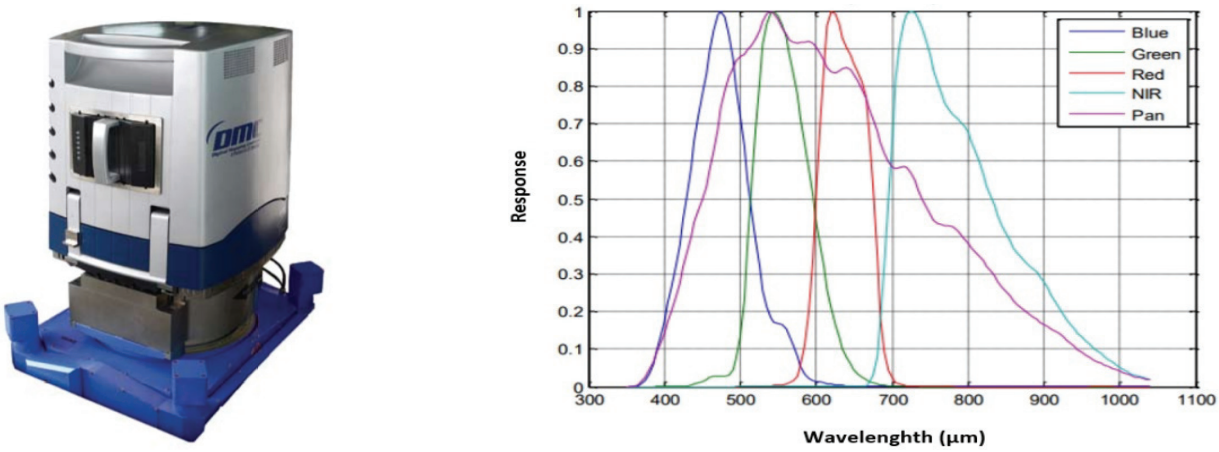

(a) **(b)**

Figure 2: Multispectral photogrammetric sensor
a) Photo of the Z/I DMC sensor - (b) Spectral response.

In order to cover the AOI, the flight planning by 11 flight lines (FLs) and 216 images have been realized. The stereoscopic coverage values adopted for this project have been: 60% of end-lap and 30% of side-lap. The images were acquired the 19th September around the 11.00 a.m. UTC time at an altitude of 2000m in clear sky conditions using Partenavia P68 Observer airborne.

B. Multispectral photogrammetry airborne sensor: Z/I DMC

The airborne sensor used for the experimentation is the Z/I DMC (Digital Mapping Camera) manufactured by Intergraph (now Hexagon group) which has a sensor size of 13824 x 7680 pixels and acquires in PAN and MS mode (Fig. 2a). Pan-sharpening task [31] is used to produce colour images with high geometric resolution. The panchromatic channel contains four 7k x 4k large-area CCD chips and high-performance lenses with 120-millimeter focal length at a maximum aperture of f/4. In addition to the PAN channel, four multi-spectral camera heads are incorporated in the camera base unit. Each colour channel has a wide-angle lens with a maximum aperture of f/4 and 25-millimeter focal length, a 3k x 2k CCD chip. These cameras are mounted inside a rigid optics frame designed specifically to ensure precise alignment of the optical axes [32]. The DMC sensor acquire in four wavelength bands: Blue (400 – 580 nm), Green (500 – 650 nm), Red (590 – 675 nm) and NIR (675 – 850 nm). The spectral radiometric response of the four bands is shown in the Fig. 2b.

C. GIS and Remote Sensing methodology

In order to build cover land map by application of the remote sensing and GIS technology [33], it was to necessary to carry out several steps, which can be summarized as follows:

- Pre-processing of the images: georeferencing and mosaic of the multispectral images.
- Image analysis: application of remote sensing techniques.
- GIS implementation to build land cover map.

Because the use of automatic algorithms, such as the *supervised* and *unsupervised*, did not provide a good classification of the territory due to the elevated detail of the thematic map, it was necessary to study an alternative approach. This approach first provides the identification of the classes that can be properly categorized with photo-interpretation and then by means of remote sensing techniques. Indeed, the first identified classes by photo-interpretation of RGB and CIR orthophoto have been the anthropic ones, such as urban and semi-urban fabric. The other classes have been identified, beyond by the photo-interpretation method, using the spectral signature and the support of NDVI and NDWI maps. In the following land classification section, it has been described how it has been possible to integrate the several information and, in some cases, the difficulty to identify some parts of the territory. Summarizing to I LEVEL of *Corine Land Cover*, the several classes and sub-classes have been determinate using an appropriate technique, as shown in the Table II.

Table II. Method used to determine an object class.

I LEVEL CLC	PHOTOINTERPRETATION		NDVI	NDWI	SPECTRAL SIGNATURE
	RGB	CIR			
1 ARTIFICIAL SURFACES	X	X	X		
2 AGRICULTURAL AREAS	X	X	X		
3 FOREST AND SEMI NATURAL AREAS	X	X	X		X
5 WATER BODIES	X			X	

D. Multispectral orthophoto

The generation of multispectral orthophoto allows to obtain, in a specific geodetic reference system, the spectral characteristics of each pixel and, as a consequence, each part of the territory observed. In addition, the possibility to obtain the External Orientation (EO), i.e. position and attitude of an image at the time of exposure by Direct Georefernceing (DG) allows the speed the photogrammetry workflow [34]. EO parameters are obtained by the integration of Global Navigation Satellite Systems (GNSS) and Inertial (IMU) measures and kinematic post-processing software. In this way, with elevate accuracy and in a short time, it is possible to obtain EO parameters. The DMC sensor has been connected to Applanix Pos AV 510 navigation system [35, 36, 37] and DGPS processing has been obtained using a master station whose maximum distance from the aircraft has been 30 km.

To improve the quality of the EO parameters, the aerial triangulation (AT) process has been performed. In this project, 5 Ground Control Points (GCP) have been inserted. The coordinates of this GCPs have been obtained by GNSS survey in Network Real Time Kinematic (NRTK) mode. The report of AT processing, generated by photogrammetric software, is reported below:

Number of Control Points:9

Number of Terrain Points:2885

Number of Images:216

Number of Cameras:1

Number of GPS Profiles:1

Number of Add. Observations: 585

RMS values of weighted residuals of X,Y and Z GPS coordinates (m)

Profile ID. 1 0.001 0.002 0.003

RMS values of weighted residuals of Omega, Phi and Kappa attitude observations (deg)

Group ID. 1 0.0018 0.0016 0.0013

A Digital Elevation Model (DEM) is required in order to create an accurate orthophoto. The DEM can be obtained in several ways: aerial stereo image [38], Airborne Laser Scanner [39, 40], radar [41]. In this case, the DEM has been obtained by stereo image and generate with a geometric resolution of 5m x 5m. The projection system chosen for the project has been Universal Transverse of Mercator (UTM) in the National geodetic reference system, which has been introduced by one Italian Minister Council Presidency Act. Also, the projection system adopted has been UTM 33N-ETRF2000. The resampling of the image, i.e. the technique that allows to attribute the values of pixels of the starting image to correct the final image cells, have been performed with the "Nearest Neighbour" algorithm because this technique has the advantage of keeping the radiance values unchanged and allows the calculation operations in a short time. The Ground Sample Distance (GSD) chosen for the orthophoto has been of 20cm. The last step, in order to build multispectral orthophoto on the AOI, has been the mosaic task. In Erdas Imagine environment, the mosaic of the 216 image has been realized.

E. Land classification and GIS project

Once the mosaic of the MS images is obtained, it is possible to calculate the NDVI index by the equation (1) using the *raster calculator* implemented in ArcGIS software. A clip of the orthophoto in RGB (Fig. 3a), in CIR (Fig. 3b) and the map of NDVI (Fig. 3c) of the following urban area is showed.

Also, thanks the use of photo-interpretation of RGB and CIR orthophoto and the support of the NDVI map, some artificial surface (urban fabric, road and rail network and associated land, mineral extraction sites, green urban and sport and leisure facilities) have been determinate. Indeed, the RGB and CIR ortophoto allows an intuitive interpretation of the urban fabric. In addition, as easy to note from the fig. 3c, NDVI index allows to emphasize the vegetation area (red colour) than other area, such as urban area (colour blue) and the soils (yellow/light blue).

(a)

(b)

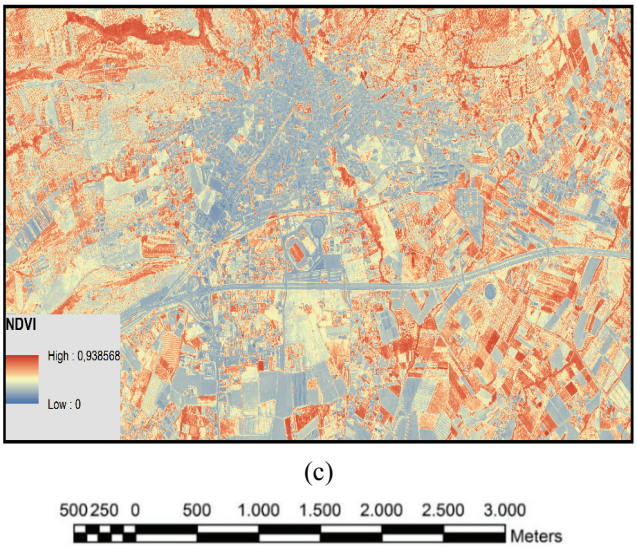

(c)

Figure 3: Clip of urban and near suburbs region in RGB (a), CIR (b) and NDVI (c) maps.

The classification of the agricultural lands has been conducted in the in the same way of the anthropic structure due to the very important presence of the protection structure such as hail nets, greenhouses, white and black films (Fig. 4). This structures did not allow the automatic recognition of the vegetation or crops. For this reason, the only way to determine this has been the photo-interpretation task and, in some cases, by terrestrial recognition. In critical cases where the land is covered by anthropic structure and the place has been inaccessible, the land information has been extracted by cadastral database.

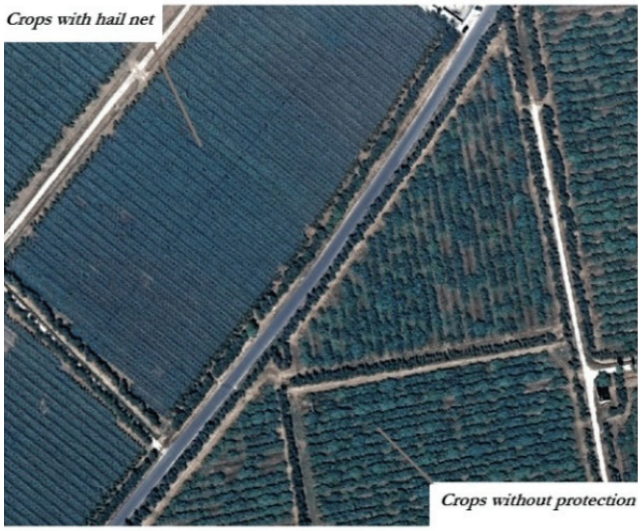

(a)

(b)

Figure 4: Example of protection structures

a) hail nets - b) several types of greenhouses

The greatest part of the agricultural area under investigation is occupied by permanently irrigated arable land. However, in this area there are also important areas with the presence of the fruit trees and olive groves; modest is the extension of vineyards.

The classification of the forest area has been realized thanks to the use of the spectral signature. In this way, it has been possible to discriminate the coniferous forest and broadleaf. Indeed, the coniferous forest has a lower reflectance than the other especially in the near infrared range. The leaf structure is responsible for spectral behaviour in nearby infrared bands. The leaf structure is the spatial organization of the leaf cells with reference to its morphological evidence that varies from one species to another. Infrared radiation does not interact with chloroplasts but is greatly influenced by the leaf structure which causes a different reflection of the incident energy [42]. Therefore, using the MS orthophoto, it has been possible to recognize the areas covered by evergreen oak forests (holm and cork oaks), Mediterranean pines and cypress forests. In particular, alder trees have been recognized along the *Sele* river, Mediterranean pines along the coastline in protection of agricultural crops and evergreen oak forests in the highest part of the territory.

As concerning the water bodies, they have been determined using the NDWI index. In this way it has been possible to determine the sea, the canal, river etc. The good result of the classification obtained using this index is shown in the Fig. 5. To extract only waterbodies, a transformation from raster to polygon has been accomplished. This task has been realized by suitable tool implemented in ArcMap software.

All the land information has been reported in a ESRI shape file (type polygon) containing the field code, description and notes in according the *Corine Lance Cover* classification. In this way the thematic map of the land cover has been obtained (Fig. 6). Subsequently, for each polygon has been calculated the surface. Summarizing to level I of the CLC, it has been possible to obtain even the distribution of the land cover of the area study. As can easily be seen from the graph (pie chart) reported in Fig. 6, the greatest part of the territory is constituted by agricultural areas (84%) and only a small part is characterized (7%) by artificial surfaces.

F. Estimation accuracy of the thematic map

The thematic maps must be subjected to a rigorous statistical assessment of accuracy before being used. The accuracy of a thematic map is defined as the measure of the agreement between the thematic map, obtained from the classification and a reference map (data truth) and it is based on the construction of the error matrix (or confusion matrix). The confusion matrix is a square matrix: the columns represent the reference data while the rows represent the classification data. In this way, the elements of the diagonal matrix represent the number of correctly classified pixels (Dii). The reference data has been obtained by ground control check and, in some areas where it is impossible to access, it has been necessary to consult other land information, such as the cadastral database. A measure for the overall classification accuracy (T) can be derived from this matrix by counting how many pixels were classified correctly and dividing this value by the total number of pixels (n) of the matrix adopting the following equation [43]:

$$T = \frac{\sum_{i=1}^{n} D_{ii}}{n} \tag{11}$$

Where $n = \sum R_i = \sum C_j$

The value *T* archived, was 98.1%.

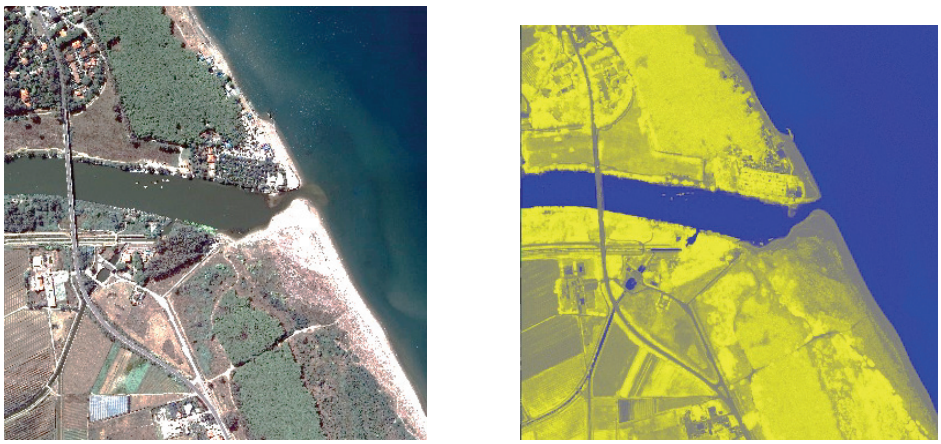

(a) (b)

Figure 5: Application of NDWI to area study

a) Clip of region in RGB - b) NDWI values in yellow-blue representation.

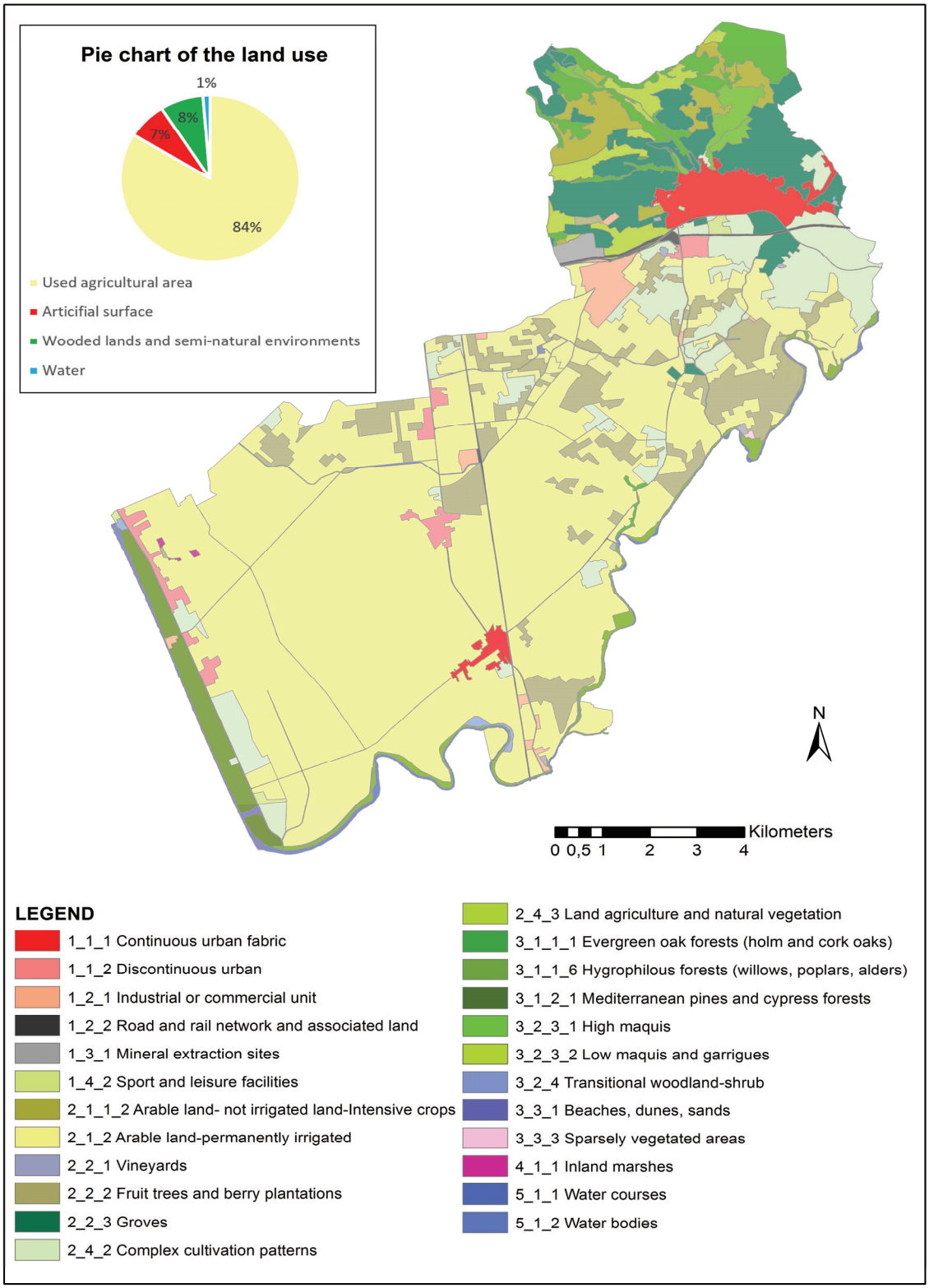

Figure 6: Land cover map (IV level) of the area study.

DISCUSSION

In order to cover the AOI, it has been necessary to realize a mosaic of all images belonging to various flight lines. However, along two adjacent FL a small diverse value of exposure has been verified. This phenomenon is more accentuated between two parallel flight lines in the case the

FLs have been acquired in opposite directions. This means that some object has a different DN value if it is observed from different frame images. Therefore, in order to overcome this inconvenience, the flight mission needs to be carefully planned if the aim of the project concerns the application in Remote Sensing environment. In other words, it is desirable to acquire the image in the same direction in order to obtain more homogeneity pixel and, of consequence, try to process the images in an automatic way.

Further, the number of images and FL needed to cover the AOI is related to the dimension of the frame of the sensor. Also, if it is necessary to cover large areas, the use of large camera sensors should minimize the problem of diverse exposure in the AOI. Of course, increasing the format of the sensors, further to obtain more colour homogeneity, the project is more efficient in terms of acquisition time and, consequently, even from the economic point of view. Indeed, in the last year, the technology developed of digital photogrammetry sensor is evolving in this direction [43], as shown in the following Table III for DMC camera:

Table III. Trend of the DMC sensors over the years.

Year	Type Model	Sensor Resolution
2003	Z/I DMC	106 Megapixel
2010	Z/I DMC II 140	140 Megapixel
2010	Z/I DMC II 230	230 Megapixel
2010	Z/I DMC II 250	250 Megapixel
2015	Leica DMC III	391 Megapixel

CONCLUSIONS

The use of the high quality of the images obtained by photogrammetric digital sensors has allowed to build multispectral orthophoto with elevated geometric resolution.

However, the use of frame sensors has presented some problems regarding the conversion from DN to reflectance and the diverse exposure of each image. This is a limit for a full integration in Remote Sensing applications. Therefore, in land cover classification with elevate detail of land objects, the photo-interpretation still plays a key role. To overcome these issues, speed up and improve the quality of the thematic map, a suitable methodology that combines image-processing methods and photo-interpretation, has been developed. Indeed, as shown in the case study, it has been possible to build a land cover map (in accordance with Corine Land Cover standard classification) with elevated grade of detail. Furthermore, the high value of accuracy on the principal diagonal of the confusion matrix shows an elevated level of classification of the several land objects and confirms the validity of the procedure adopted.

Lastly, the management of the information by GIS software has enabled an efficient environment for the representation and analysis of the land cover distribution.

REFERENCES

[1] Everitt, J. H.; Escobar, D. E.; Appel, D. N.; Riggs, W. G.; and Davis, M. R. (1999). Using airborne digital imagery for detecting oak wilt disease. Plant disease, 83(6), 502-505.

[2] King, D. J. (2000). Airborne remote sensing in forestry: sensors, analysis and applications. The Forestry Chronicle, 76(6), 859-876.

[3] McGlone, C. Manual of Photogrammetry “Aerial film cameras“, 6th ed.; ASPRS: Bethesda, MD, USA, 2013, pp.99-99.

[4] Boland, J., T.; Ager, E.; Edwards, E.; Frey, Toth, C.; Walker, S., Whittaker, E., Zavattero P.; and Zuegge H. (2004). "Camera and sensing systems“ (Chapter 8). Manual of Photogrammetry, Fifth Edition, American Society for Photogrammetry and Remote Sensing (edited by McGlone, J.C., Mikhail E.M., and J. Bethel), pp 587-590.

[5] Stow, D.; Coulter, L.; and Benkelman, C. (2009). “Airborne digital multispectral imaging”. SAGE Publications, London.

[6] Petrie, G.; and Walker, A. S. (2007). Airborne digital imaging technology: a new overview. The Photogrammetric Record, 22(119), 203-225.

[7] Kellenberger, Tobias, W.; and Nagy, Patrick. (2008) Potential of the ADS40 aerial scanner for archaeological prospection in Rheinau, Switzerland, The International Archives of the Photogrammetry, Remote Sensing and Spatial Information Sciences. Vol. XXXVII. Part B4.

[8] Gruber, M.; Ponticelli, M.; Bernögger, S.; and Leberl, F. (2008). UltraCamX, the large format digital aerial camera system by Vexcel Imaging/Microsoft. In Proceedings of ISPRS XXIst Congress “Silk Road for Information from Imagery. 3-11.

[9] Koschke, L.; Fürst, C.; Frank, S.; and Makeschin, F. (2012). A multi-criteria approach for an integrated land-cover-based assessment of ecosystem services provision to support landscape planning. Ecological Indicators, 21, 54-66.

[10] Toure, S. I.; Stow, D. A.; Weeks, J. R.; and Kumar, S. (2013). Histogram curve matching approaches for object-based image classification of land cover and land use. Photogrammetric Engineering & Remote Sensing, 79(5), 433-440.

[11] Weichelt, H.; Wagnera, B.; and Klaedtkeb, H. G. (2005). Remote Sensing Approach For Digital Aerial

Imagery. In ISPRS Hannover Workshop 2005.

[12] Dzieszko, M.; Dzieszko, P.; and Królewicz, S. (2012). Digital aerial images land cover classification based on vegetation indices. Quaestiones Geographicae, 31(3), 5-23.

[13] Blasi, C., Capotorti, G., Copiz, R., Guida, D., Mollo, B., Smiraglia, D., & Zavattero, L. (2014). Classification and mapping of the ecoregions of Italy. Plant Biosystems-An International Journal Dealing with all Aspects of Plant Biology, 148(6), 1255-1345.

[14] Yüksel, A., Akay, A. E., & Gundogan, R. (2008). Using ASTER imagery in land use/cover classification of eastern Mediterranean landscapes according to CORINE land cover project. Sensors, 8(2), 1237-1251.

[15] Apollonio, C.; Balacco, G.; Novelli, A.; Tarantino, E.; and Piccinni, A. F. (2016). Land use change impact on flooding areas: The case study of Cervaro basin (Italy). Sustainability, 8(10), 996.

[16] Akar, Ö. (2017). Mapping land use with using Rotation Forest algorithm from UAV images. European Journal of Remote Sensing, 50(1), 269-279.

[17] Bossler, J. D.; Jensen, J. R.; McMaster, R. B.; and Rizos, C. (Eds.). (2004). Manual of geospatial science and technology. CRC Press.

[18] Brivio, P. A.; Zilioli, E.; and Lechi, G. L. (2006). Principi e metodi di telerilevamento. CittaStudi, 434-435.

[19] Gao, B. C. (1996). NDWI—A normalized difference water index for remote sensing of vegetation liquid water from space. Remote sensing of environment, 58(3), 257-266.

[20] Tucker, C. J. (1979). Red and photographic infrared linear combinations for monitoring vegetation. Remote sensing of Environment, 8(2), 127-150.

[21] McFeeters, S.K. The use of the Normalized Difference Water Index (NDWI) in the delineation of open water features. Int. J. Remote Sens. 1996, 17, 1425–1432.

[22] Gitelson, A. A., & Merzlyak, M. N. (1997). Remote estimation of chlorophyll content in higher plant leaves. International Journal of Remote Sensing, 18(12), 2691-2697.

[23] Blackburn, G. A. (1998). Quantifying chlorophylls and caroteniods at leaf and canopy scales: An evaluation of some hyperspectral approaches. Remote sensing of environment, 66(3), 273-285.

[24] Le Maire, G.; Francois, C.; and Dufrene, E. (2004). Towards universal broad leaf chlorophyll indices using PROSPECT simulated database and hyperspectral reflectance measurements. Remote sensing of environment, 89(1), 1-28.

[25] Peña‐Barragán, J. M.; López‐Granados, F.; Jurado‐Expósito, M.; and García‐Torres, L. (2006). Spectral Discrimination Of Ridolfia Segetum And Sunflower As Affected By Phenological Stage. Weed Research, 46(1), 10-21.

[26] Markelin, L.; E. Honkavaara, J.; Peltoniemi, E.; Ahokas, J.; Hyyppä, R.; Kuittinen, J.; and Suomalainen. (2008). Radiometric calibration and characterization of large-format digital photogrammetric sensors in a test field. Photogrammetric Engineering & Remote Sensing, vol. 74, number 12, 1487-1500.

[27] Cocks, T.; Jenssen, R.; Stewart, A.; Wilson, I.; and Shields, T. (1998). The HyMapTM airborne hyperspectral sensor: the system, calibration and performance. In Proceedings of the 1st EARSeL workshop on Imaging Spectroscopy. 37-42.

[28] Martínez, L., Arbiol, R., Palà, V., & Pérez, F. (2007). Digital Metric Camera radiometric and colorimetric calibration with simultaneous CASI imagery to a CIE Standard Observer based colour space. In Geoscience and Remote Sensing Symposium, 2007. IGARSS 2007. IEEE International. 4140-4143.

[29] B.-C. Gao, M.J. Montes, Z. Ahmad, C.O. (2000) Davis Atmospheric correction algorithm for hyperspectral remote sensing of ocean color from space, Applied Optics, 39, 887–896.

[30] Ryan, R. E.; Pagnutti, Mary. (2009) Enhanced Absolute and Relative Radiometric Calibration for Digital Aerial Cameras, Photogrammetric Week, 2009, 81-90.

[31] Parente, C.; and Pepe, M. (2017). Influence of the weights in IHS and Brovey methods for pan-sharpening WorldView-3 satellite images. International Journal of Engineering & Technology, 6(3), 71-77.

[32] Hinz, A.; Dörstel, C.; and Heier, H. (2001). DMC-The digital sensor technology of Z/I-Imaging. In In D. Fritsch and R. Spiller (eds) Photogrammetric Week'01.

[33] Pepe, M.; and Parente, C. (2017). Cultural Heritage Documentation in Sis Environment: an application for "Porta Sirena" in the archaeological site of Paestum. In International Archives of the Photogrammetry, Remote Sensing & Spatial Information Sciences, 42.

[34] Cramer M., (2010). Direct georeferncing using GPS/INERTIAL exterior orientations for

photogrammetric applications. International Archives of Photogrammetry and Remote Sensing, Amsterdam, Holland, 33, 198–205.

[35] Mostafa, M.; Hutton, J.; and Reid, B. (2001). GPS/IMU products-the Applanix approach. In Photogrammetric Week. Vol. 1, pp. 63-83.

[36] Pepe, M.; Prezioso, G.; and Santamaria, R. (2015). Impact of vertical deflection on direct georeferencing of airborne images. Survey Review, 47(340), 71-76.

[37] Pepe M., Prezioso G., (2016). Two Approaches for Dense DSM Generation from Aerial Digital Oblique Camera System, in Proceedings of the 2nd International Conference on Geographical Information Systems Theory, Applications and Management, 63-70.

[38] Ismail, Z.; and Jaafar, J. (2013). DEM derived from photogrammetric generated DSM using morphological filter. In Control and System Graduate Research Colloquium (ICSGRC), 2013 IEEE 4th. pp. 103-106.

[39] Ma, R. (2005). DEM generation and building detection from lidar data. Photogrammetric Engineering & Remote Sensing, 71(7), 847-854.

[40] Pepe, M. (2017). A survey by Airborne Laser Scanner of open large structure: A case study of Pompeii Amphitheatre, ARPN Journal of Engineering and Applied Sciences, 12(21), 1-11.

[41] Farr, T., G., and Kobrick, M. (2000). Shuttle Radar Topography Mission produces a wealth of data. Eos, Transactions American Geophysical Union, 81(48), 583-585.

[42] Campbell, J. B. (2007). Introduction to Remote Sensing (4th edn). The Guilford Press, New York, NY.

[43] Bogoliubova, A.; and Tymków, P. (2014). Accuracy assessment of automatic image processing for land cover classification of St. Petersburg protected area. Acta Scientiarum Polonorum. Geodesia et Descriptio Terrarum, 13, 1-2.

[44] Neumann, Klaus; Welzenbach, Martin; and Timm Martin. (2016). CMOS imaging sensor technology for aerial mapping cameras, Int. Arch. Photogramm. Remote Sens. Spatial Inf. Sci., XLI-B1, 69-2, doi:10.5194/isprs-archives-XLI-B1-69.